Solar-Powered EV Charging System with G2V and V2G Charging Configuration

Dr Sheik Mohammed S [1,*], Dr Mohammed Mansoor O [2,$], Dr Ulaganathan M [3,#]
[1 2]Assistant Professor, TKM College of Engineering, Kollam, Kerala, India
[3]Assistant Professor, PSN College of Engineering, Tirunelveli, Tamil Nādu, India
[*]ssheikmd@yahoo.co.in, [$]mansooreee@tkmce.ac.in, [#]ulagu.er@gmail.com

Abstract

Fuel consumption has increased drastically in the transport sector than in other sectors like agriculture, industries, etc., and the transportation sector is one of the prime sources of CO_2 emission. Under these crucial circumstances, the transport sector has started adopting clean energy strategies as a mission, which leads to the shift towards Electric Vehicles (EV) to reduce the ever-rising pollution and its detrimental effect on the environment. EV-based transportation faces predominant challenges due to the lack of charging infrastructures. Further, the source of power for the charging stations is from the fossil fuel-based power generating grids. Solar energy is one form of clean energy, which can be used as an alternative power source in EV charging stations. This chapter presents and discusses a solar energy-powered EV charging station designed in V2G and G2V configurations. The proposed EV charging station is developed with different topologies of the power converter, which is more suitable to operate the charging station efficiently. The EMS system effectively controls the converters and the energy storage unit operation to maintain the power-sharing between the components. The simulation of the charging station is done on the MATLAB / Simulink software. The performance of the developed charging station is evaluated by conducting ripple analysis on the converter for different input conditions. The simulation results reveal EMS performance and the importance of designing optimal power converters in developing the solar-powered charging station.

Keywords: Electric Vehicle, Charging, Vehicle to Grid (V2G), Grid to Vehicle (G2V), Solar Power, DC-DC Converters

1. INTRODUCTION

Worldwide energy consumption is steadily increasing every year. By the end of 2019, 419 million Tera Joules (TJ) of energy had been consumed by various sectors like industries, transport, residential, etc. The transport sector is the second-largest energy consumer, with nearly 121 million TJ of energy occupied, as depicted in Fig. 1 [1]. Almost 90 % of the transport sector's energy consumption is met from petroleum byproducts, shown in Fig. 2. The increasing population and enormous development in the transport sector accelerated the fossil fuel requirement and hiked its price. In addition, the transport sector is one of the top emitters of Greenhouse gases that emit 7.3 GT of CO_2 in the year 2020 [2]. Fossil fuels not only lead to environmental pollution, but also their availability is reducing day by day. Currently, most conventional vehicles use Internal Combustion Engine (ICE). ICE uses fossil fuels as a driving source and exhausts harmful CO_2 into the environment, which leads to global warming. A promising alternative to the ICE is the transport sector electrification using Battery-operated Electric vehicles (B-EVs). The B-EVs doesn't only limit fossil fuel usage, but also drastically reduce greenhouse gas emissions.

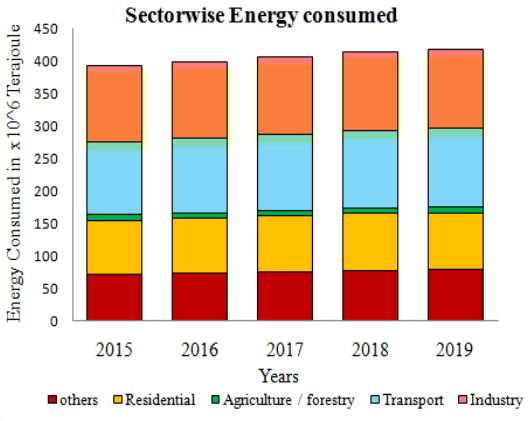

Fig. 1 Sector wise Energy consumed [1]

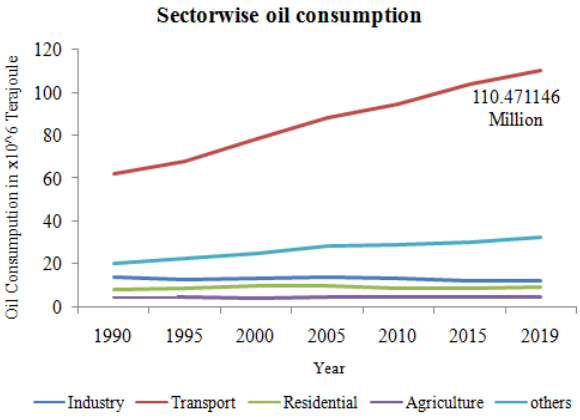

Fig. 2 Oil consumption by transport sector [1]

The EV technology has seen significant progress in the past decade, and it is a promising solution to reduce CO_2 emissions and improve power quality in power distribution systems. A typical Battery Electric Vehicle (B-EV) includes an electric motor acting as propulsion energized by a storage unit, especially with a battery [3]. In addition, B-EV consists of the DC-DC power converter to regulate and control the power delivered to the electric motor. The growth in EV technology synergies the EV manufacturers and electricity service providers in the EV charging domain. The EV can be charged through DC or AC systems. EV batteries are currently charged by conductive and inductive charging at

conventional power outlets or charging stations [4]. The EV charging station may affect the power distribution system by loading the grid due to a poorly designed charging station [5].

The electricity sources used to charge the batteries in the EV define the benefits its emission reduction. EVs become emission-free only when they are charged from renewable energy sources like solar power, wind power, etc., [6]. However, the Renewable Energy (RE) source penetration affects the power grid due to its unpredictable electricity supply. The energy storage system can stabilize the variable electricity generated by the resources by storing or supplying the electricity into the grid [7]. Similarly, the EV batteries can act as an energy storage system, enabling EVs to charge the battery through electricity from the RE sources and export the power to the grid, commonly named the V2G operation [8].

With the increasing need for EV charging stations, solar PV power is probable gaining interest in the parking slot charging facilities and meet grid demand. Feasibility studies in implementing rooftop PV systems to charge the EV storage unit showed promising results [9, 10]. The combined possibility of V2G operation in the EV, and power generation from PV systems, enables the avenues for optimal power generation scheduling is reported in [11]. The results conclude that the proposed system attains minimal grid operating cost and improves the grid operation. Detailed analysis on the EV charging point and integration of solar rooftop is discussed in [12]. The reported study reveals the interaction in the EV charging station powered by a large solar PV rooftop and distribution system. The proposed model reduced the fluctuations in grid voltage by 15% and met the grid demand through V2G support. An extensive review on the solar-power car charging station in the Frauenfeld city of Swiss is reported in [13], which brought out the benefits of solar power parking station that covers the EV energy demand up to 40 %.

Hassan Fathabadi [14] proposed a solar-powered EV charging station with V2G support and connected to the grid, including PV array, Maximum Power Point Tracking (MPPT) Controller, bi-directional DC/DC converter, and bi-directional inverter. In [15], a solar-powered EV charging station architecture that integrates microgrid and AC grid is discussed.

2 Architecture of Solar-powered EV charging station

The architecture of EV charging station is shown in Fig. 3, which supports two EV charging configurations: Grid to Vehicle (G2V) and Vehicle to Grid (V2G). The entire

charging station is a DC system. Therefore, DC microgrid is chosen, which acts as a small-

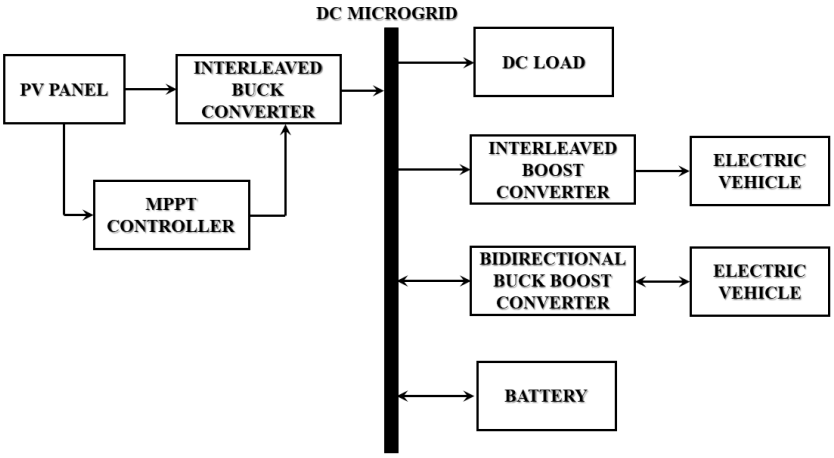

Fig. 3 Block diagram representation of the Architecture of Solar-powered EV charging

scale grid. This DC microgrid includes the PV system and an energy storage system. The output power from the PV system is utilized to charge the EV and handle the DC load. The battery in the architecture is employed to store the excess power generated by the PV system. The various converter topologies in the charging station are monitored and controlled by the Energy Management System (EMS). To ensure the controlled and reliable operation of the system, EMS monitors the PV power generation, battery, and EVs State of Charge (SOC). In turn, EMS ensures continuous DC power supply in the microgrid by regulating the converters in the charging station.

The DC microgrid voltage level in this architecture is 48 V. A 1 kW solar PV system is considered as the source of the charging station connected. Solar PV system connected with the DC grid via interleaved buck converter. The PV system has maximum output voltage of 122.8 V, which is stepped down by the interleaved buck converter to the microgrid voltage level of 48 V. Under varying irradiation conditions, PV system power output is maximized by variable step size P&O MPPT controller. The interleaved boost converter boosts the microgrid bus voltage to 72 V for charging the EV which operates only in G2V configuration. The interleaved buck-boost converter supports both G2V and V2G connection configuration, which charges the EV in boost mode and discharges the EV battery in buck mode.

The PV power generation, SOC of the microgrid - connected battery, and EV battery decides mode of operation of the proposed charging station. In Mode 1, The PV system produces sufficient energy to charge the EV. Hence, EV battery is directly charged from PV source, as depicted in Fig 4 (a). Mode 2 as depicted in Fig 4 (b) is possible when the PV

system is self-stained to generate power, which makes the system to charge EV battery and meet the DC load demand can be met. In Fig 4 (c), the mode enables the system to handle the only DC load with available PV power. The battery connected to DC microgrid acts as an energy storage system in the charging station to store the generated PV power in the absence of EV battery charging and DC load. Mode 4, charging of energy storage system during the no load condition is shown in Fig 4 (d). When the PV power generation is insufficient to charge the EV, mode 5 in Fig 4(e) is adopted. In mode 6, EV is charged with the support of a battery connected to a DC microgrid. Under reduced PV power generation, the DC load demand is balanced with the energy stored in the EV battery unit working in V2G configuration as represented in Fig 4 (f). Mode 7, illustrated in Fig.4 (g) enables the DC microgrid to meet the DC load requirement with the energy storage system connected during insufficient power generation in the PV

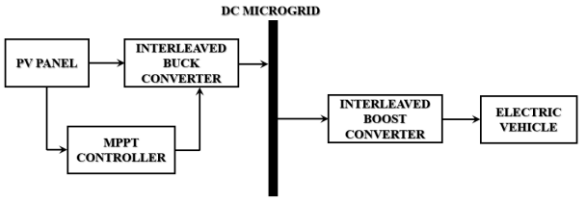

Fig 4 (a) Mode 1

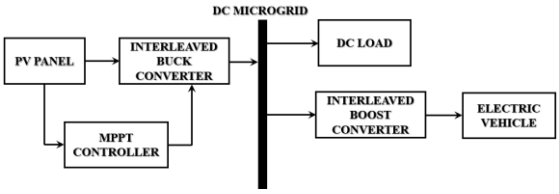

Fig 4 (b) Mode 2

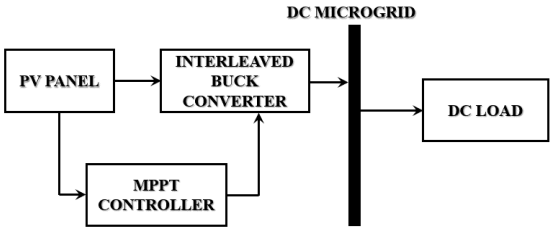

Fig 4 (c) Mode 3

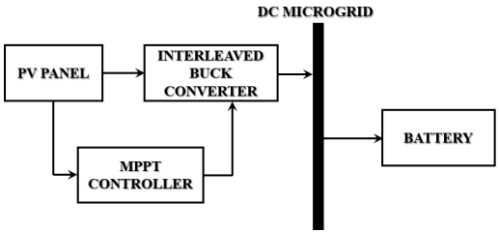

Fig 4 (d) Mode 4

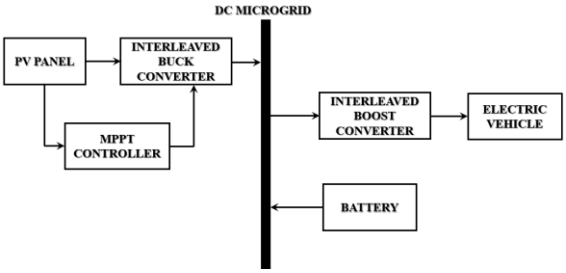

Fig 4 (e) Mode 5

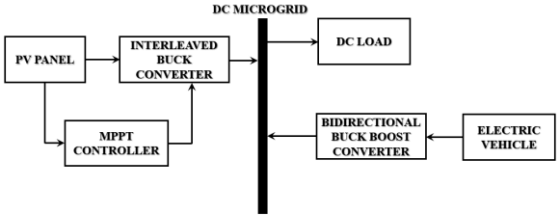

Fig 4 (f) Mode 6

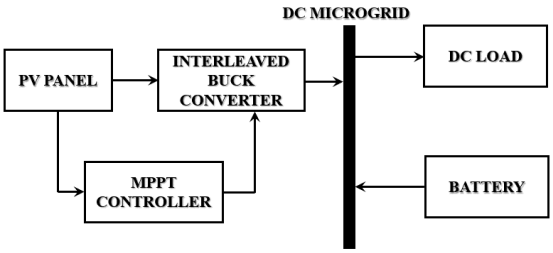

Fig 4 (g) Mode 7

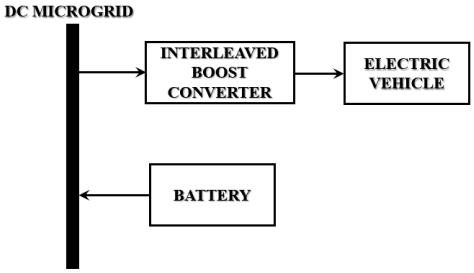

Fig 4 (h) Mode 8

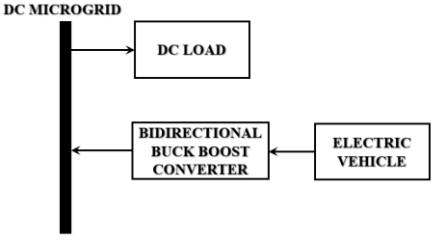

Fig 4 (i) Mode 9

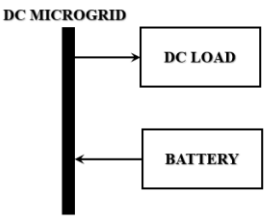

Fig 4 (j) Mode 10

Fig 4. Operating Modes of the Solar Powered Electric Vehicle Charging Station

system. In mode 8, the EV is charged with energy stored in the microgrid-connected battery during the nighttime, which is shown in Fig. 4(h). Under no PV power generation, the DC

load power requirement is managed as shown in Fig 4 (i) and Fig 4 (j) with the energy stored in the EVs and storage batteries.

3 Design converters for the Solar-powered charging station

3.1 Two-phased interleaved Buck converter design for solar PV system:

A 1-kWp PV array is considered in this study. It includes four 250 W PV modules connected in series. The specification of the 250 W PV module is given in Table 1.

Table 1. 250 W PV module specification

PARAMETER	SPECIFICATION
Open circuit voltage	122.8 V
Short Circuit Current	8.66 A
Maximum Power output	1000 W
Voltage at Maximum Power	116 V
Current at Maximum Power	7.35 A

The PV array voltage has to be brought to the voltage level of 48 V which is the DC microgrid bus voltage. Here, interleaved buck converter is used to integrate the PV array to the grid. The interleaved converter is a converter type that connects the "*n*" number of same-sized converters in parallel, as illustrated in Fig 5. The converter's output filter size could be downscaled because "*n*" converters are switched with the driving signal phase-shifted by $2\pi/ n$ to one another. Interleaved topology has reduced ripple in input current and output voltage when compared to conventional converter.

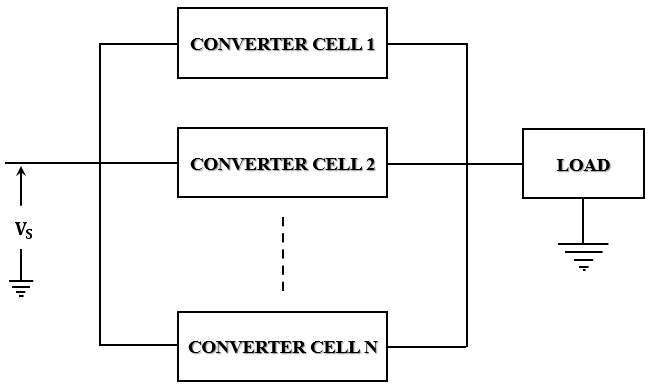

Fig. 5 Block diagram representation of the interleaved converter [16].

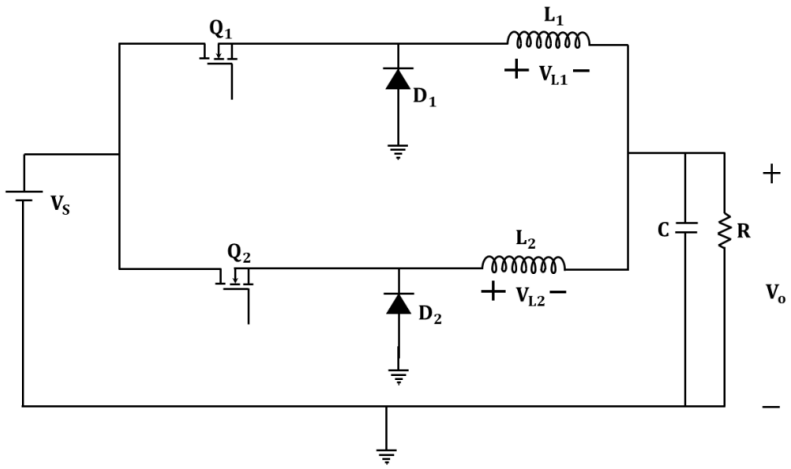

Fig. 6. Two-phase Interleaved buck converter [16].

This architecture adopts a two-phase interleaved buck converter, as shown in Fig. 6, consisting of two converters connected in parallel. The two switches are fired at an angle of 180^{o} phase shift, and at the constant switching frequency. The PV power is transferred to the microgrid by an interleaved buck converter. The interleaved buck converter is designed to scale down the PV array output of 122.8 V to grid 48 V. The converter's components and its duty cycle are calculated using the Eq. (1) - Eq. (3) tabulated in Table 2.

$$L = \frac{V_O(1-D)}{\Delta I_L f} \tag{1}$$

$$C = \frac{V_O(1-D)}{8Lf^2\Delta V_C} \tag{2}$$

$$D = \frac{V_O}{V_S} \tag{3}$$

Table 2. Interleaved Buck Converter specifications

PARAMETER	SPECIFICATION
Input voltage (V_S)	122.8V
Output voltage (V_0)	48V
Output Power	1 kW
Switching frequency f_S	20kHz
Duty ratio D	0.39
Inductance L_1=L_2	3595µH
Capacitor C	5.302µF
Capacitor voltage ripple ΔV_C	1%
Inductor current ripple ΔI_L	5%

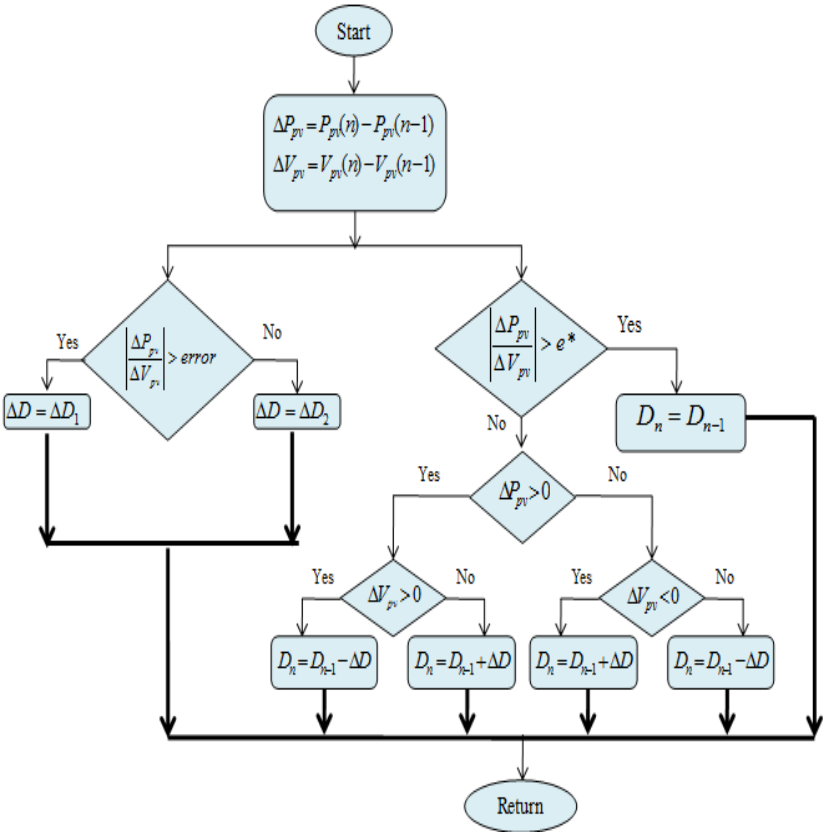

Fig. 7. Variable Step-Size P&O Algorithm Flowchart [17]

Under varying irradiation and temperature, it isn't easy to track the maximum power delivered by the PV array. Therefore, to track the maximum power point of the PV array, an MPPT controller is installed. A Variable step-size Perturb and observe (VSS - P&O) MPPT controller is used in this proposed charging station architecture, enhancing the tracking speed and reducing the maximum power point oscillation. Fig. 7 represents the flowchart of VSS P&O MPPT [9].

3.2 Interleaved boost converter for charging EV

The voltage level of EV battery taken into account for this study is 72V. Conventional boost converter boosts a DC voltage to high voltage; however, the two-phase interleaved boost converter is chosen to reduce the ripple in input current and output voltage. PI controller is used to control the duty cycle of the converter. The components of the converter are designed using Eq. (4) and Eq. (5). The designed component sizing of the 2-phase interleaved boost converter is given in Table 3.

$$L = \frac{V_S D}{\Delta I_L f} \tag{4}$$

$$C = \frac{I_O D}{f \Delta V_C} \tag{5}$$

$$D = 1 - \frac{V_S}{V_O} \tag{6}$$

Table 3. Interleaved Boost Converter specifications

PARAMETER	**SPECIFICATION**
converter Source voltage (V_S)	48V
converter Source V_o	72V
Converter Output Power	500W
Switching Frequency f_S	20kHz
Duty Ratio D	0.34
Inductor L_1=L_2	783µH
Capacitor C	327.9µF
ΔV_C	1%
ΔI_L	5%

3.3 Bidirectional Buck-Boost Converter for V2G charging configuration

The charging station proposed in this chapter allows the EV battery to act as an alternative power supply to meet the DC load demand during the PV system's inability. This V2G configuration is possible with the bidirectional buck-boost converter, which allows the power flow from grid to vehicle and vehicle to grid. Suppose if the PV array cannot deliver the required microgrid power, the bidirectional converter operates in a buck mode to scale down the EV battery voltage to the grid voltage of 48 V and transfer the energy to the grid. The bidirectional converter operates in boost mode to boost the grid voltage to EV battery voltage of 72 V during EV charging. The components of the bi-directional converter are designed with the help of the Eq. (7) - Eq. (11), .and it is listed in Table 4.

Boost mode configuration

$$V_H = \frac{1}{1-D} V_L \tag{7}$$

$$L_m = \frac{D(1-D)^2 R_H}{2f} \tag{8}$$

$$C_H = \frac{D}{R_H f (\frac{\Delta V_H}{V_H})} \tag{9}$$

Buck mode configuration

$$V_H = \frac{V_L}{D} \tag{10}$$

$$C_L = \frac{V_L(1-D)}{8\Delta V_L L_m f^2} \tag{11}$$

Table 4. Bidirectional Converter specifications

PARAMETER	SPECIFICATION
V_L	48V
V_H	72V
Output Power	500W
f_S	20kHz
D_{boost}	0.34
D_{buck}	0.66
L_m	38.388µH
C_L	276.779µF
C_H	163.966 µF
$\Delta V_H = \Delta V_L$	1%

3.4 Energy Management System developed for the Charging Station

An Energy Management System (EMS) is designed to maintain the uninterrupted power flow among the EV battery, storage battery, and DC load. The EMS continuously monitors the parameters like PV array power output (P_{PV}), DC load power (P_L), G2V EV battery charging power (P_{G2V}), State of Charge (SOC) of grid-connected battery B_{SOC} and EV battery EVB_{SOC} (SOC in V2G charging mode) to select the appropriate mode.

Steps involved in the EMS

1. Measure, the P_{PV}, P_L, P_{G2V}, $B_{SOC,}$ and EVB_{SOC}.
2. Calculates the grid power demand $P_T = P_{PV} - P_L - P_{G2V}$
3. Ensure that P_T is less than or equal to zero, then if it is yes proceeded to step 4. Else, move to step 5.
4. Ensure if B_{SOC} and EVB_{SOC} charge level is more than 30 %, then if Yes, go-to step 6 else step 7.
5. Ensure if $B_{SOC,}$ and EVB_{SOC} charge level is less than 80 %, then if Yes, go to step 8 else step 9.
6. Transfer the power stored in battery and EV battery
7. Suppose if EVB_{SOC} charge level is more than 30 %, then if Yes, continue to step 10 otherwise proceed to step 11
8. Charge both the battery in the grid and EV.

9. Check if B_{SOC} is less than 80% and EVB_{VSOC} is greater than 80%. If it goes to step 12 else go to step 13
10. Discharge the EV battery
11. Charge both the battery in the grid and EV.
12. Charge the battery and discharge EV battery.
13. Discharge battery and charge EV battery.

3.5 RIPPLE ANALYSIS

DC-DC converters are used in various applications, especially those involve battery-operated systems. Interleaved buck and interleaved boost converters are used in the proposed architecture to step down and step up the voltage to the desired level. The Interleaved converter has reduced input current and output voltage ripple, low switching loss, and faster transient response. Although the converter topology has more inductors increasing the complexity of the converter correlated to the classical DC to DC converter, it is chosen because of the low ripple content in the input and output sides [13].

Ripple analysis is conducted for both interleaved and conventional converters, and the results obtained are presented and analyzed. The input current ripple, output voltage ripple, and output power ripple for buck and boost converters are calculated. The results obtained prove that the ripple percentage of interleaved converters is less when compared with the conventional converters, which makes the proposed system more efficient and reliable when compared with a system consisting of conventional converters. The average ripple, and ripple percentage are calculated using the following formulae:

$$I_{avg} = \frac{I_{\max} + I_{\min}}{2} \tag{12}$$

$$I_{ripple} = I_{\max} - I_{\min} \tag{13}$$

$$Ripple\% = \frac{I_{ripple}}{I_{avg}} \times 100 \tag{14}$$

Here, I_{max} and I_{min} represent the maximum and minimum values of current, respectively. I_{avg} and I_{ripple} represent the average value and ripple value of current, respectively. The same formulae are used for calculating the average and ripple percentage of output voltage and output power.

3.6 Ripple Analysis of Conventional and Interleaved Buck Converters

The ripple analysis between the buck converter and interleaved buck converter is carried with the PV system. A simulation model is developed with the PV array and interleaved buck converter with the Variable Step P&O MPPT.

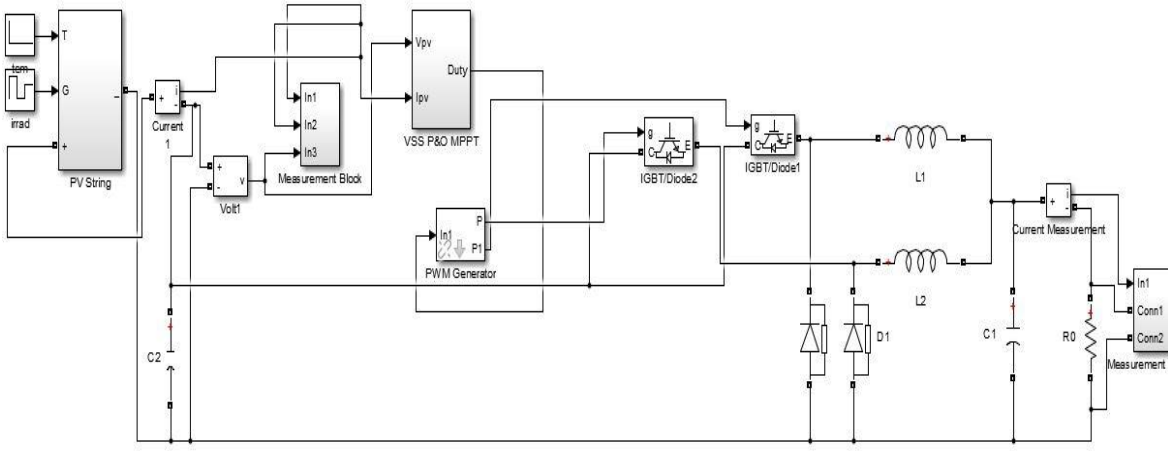

Fig 8. Simulation model of Interleaved Buck Converter

The input is varied by varying the irradiance values as 1000W/m^2, 750W/m^2, 800W/m^2 and 950W/m^2. The simulation model of the interleaved buck converter is shown in Fig 8. The ripple analysis between buck and interleaved is calculated and tabulated in Table 5.

Table 5. Ripple Analysis of conventional buck converter and Interleaved Buck Converter

Interleaved Buck Converter						**Buck converter**					
OUTPUT POWER (W)		**INPUT CURRENT (A)**		**OUTPUT VOLTAGE (V)**		**OUTPUT POWER (W)**		**INPUT CURRENT (A)**		**OUTPUT VOLTAGE (V)**	
Avg.	**Ripple%**	**Avg.**	**Ripple %**	**Avg.**	**Ripple %**	**Avg.**	**Ripple %**	**Avg.**	**Ripple %**	**Avg.**	**Ripple %**
975.8	0.286	8.25	0.66	47.41	0.147	974.5	1.8	8.33	3.406	47.38	0.9
728.1	0.466	6.21	0.77	40.95	0.268	730.35	2.04	6.23	2.74	41.04	0.9
775.85	0.425	6.57	0.76	42.28	0.236	779	2.02	6.68	2.93	42.37	0.96
925.15	0.356	7.81	0.64	46.17	0.173	924.95	1.89	7.92	3.29	46.17	0.9

Fig 9. shows the maximum power tracked by buck and interleaved buck converter. The power output of buck converters is oscillating around the MPP around ±10 W and has a maximum ripple of 2%. However, the interleaved buck converter exhibits ±2 W oscillation around the MPP and the ripple is 0.4 %.

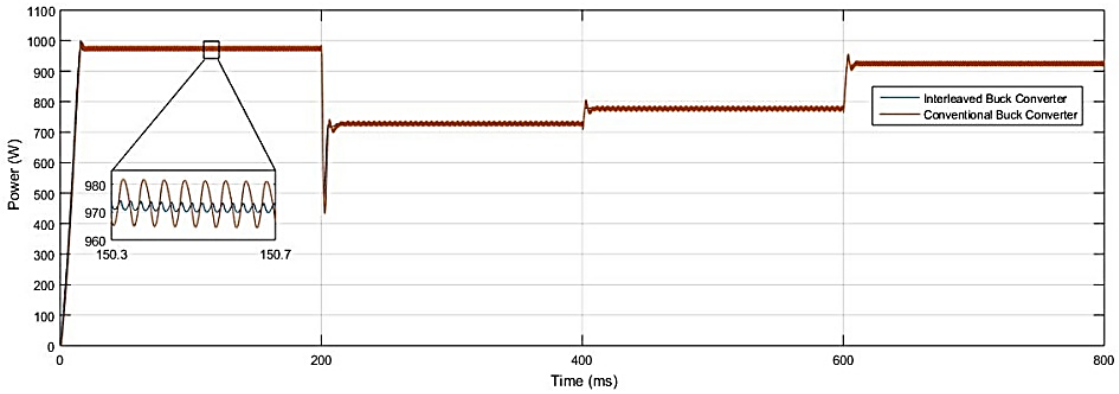

Fig 9. Maximum power output of conventional and interleaved buck converter

3.7 Ripple Analysis of Conventional and Interleaved Boost Converter

The simulation model of an interleaved boost converter is shown in figure 10. A variable DC source is used to vary the input and a PI controller is used to maintain the output voltage at 72V. The input is varied as 60V, 48V, 54V and 50V.

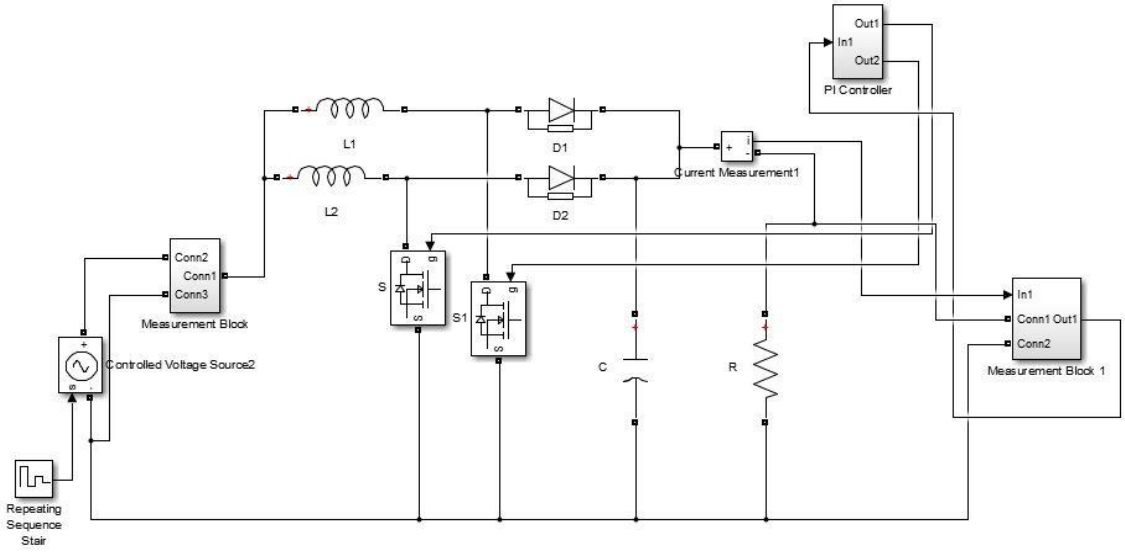

Fig 10. Simulation Model of Interleaved Boost Converter

Fig 11. shows the maximum power tracked by boost and interleaved boost converter. The power output of boost converters is oscillating around the MPP around ±5 W and has a maximum ripple of 1.02 %. Similarly, the interleaved buck converter exhibits ±1 W oscillation around the MPP and the ripple is 0.28 %. Ripple analysis is presented in Table 6.

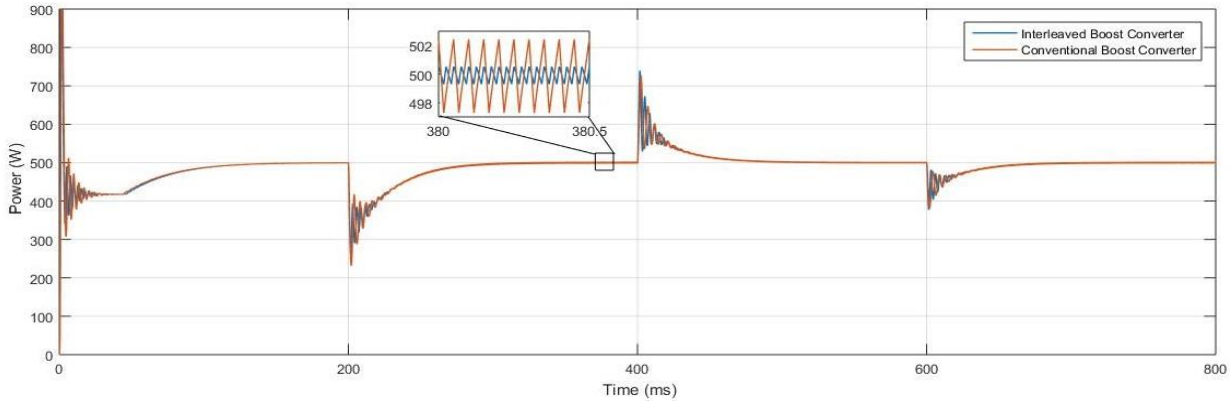

Fig 11. Power output of conventional and interleaved boost converter

Table 6. Ripple Analysis between Interleaved boost Converter and boost converter

Interleaved boost converter						**Boost converter**					
OUTPUT POWER (W)		**INPUT CURRENT (A)**		**OUTPUT VOLTAGE (V)**		**OUTPUT POWER (W)**		**INPUT CURRENT (A)**		**OUTPUT VOLTAGE (V)**	
Avg.	Ripple %	Avg.	Ripple %	Avg.	Ripple %	Avg.	Ripple %	Avg.	Ripple %	Avg.	Ripple %
499.2	0.2	8.459	5.79	71.94	0.097	498.95	0.5	8.469	7.2	71.915	0.264
500	0.2	10.73	3.35	71.99	0.097	499.85	1.02	10.685	9.265	71.99	0.5
500	0.28	9.478	5.5	72	0.097	500	0.8	9.45	9.45	72.01	0.36
500	0.24	10.25	4.8	72	0.11	499.9	0.96	10.262	8.92	72	0.46

4 Results and Discussion

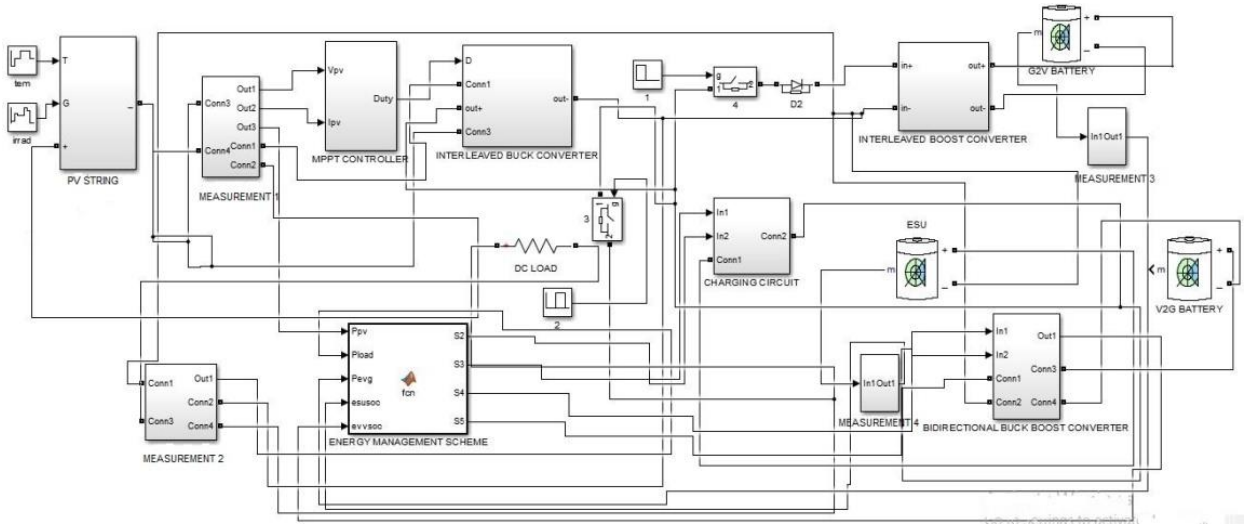

Fig 12. Simulation Model of EV Charging station

A snapshot of simulation model of the proposed system is shown in Fig.12. Simulation was carried out for varying irradiation conditions at constant temperature. The proposed model is simulated with varying input and load conditions. The model is studied with both V2G and G2V strategy with ESU.

The irradiation pattern considered is shown in Fig. 13. The values applied for the seven-time intervals are 447W/m^2, 616W/m^2, 575W/m^2, 580W/m^2, 770W/m^2, 705W/m^2 and 400W/m^2, respectively.

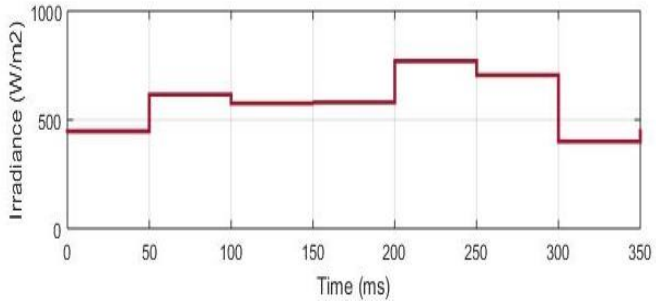

Fig. 13 Irradiance level

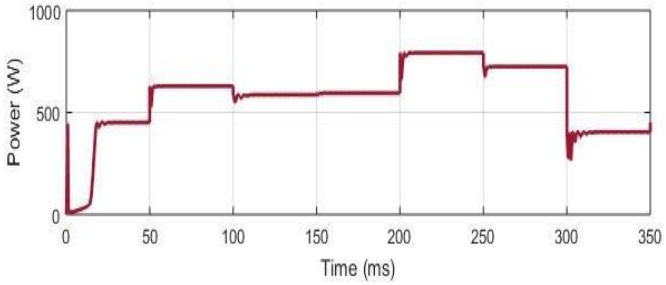

Fig. 14 PV Output Power

Fig. 14 depicts the change in PV output power, according to the change in the input irradiance conditions. The objective of the controller is effectively switch between the source, ESU, V2G and G2V loads in such a way to maintain the overall grid demand. The DC load pattern applied is shown in Fig. 15. From the figure, it can be seen that a load of 600W is applied between 150 and 300 ms.

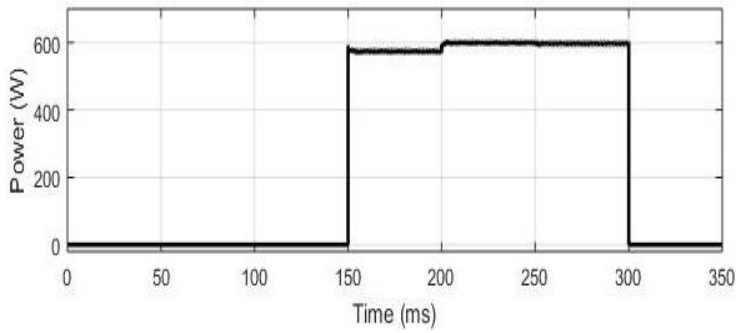

Fig. 15 DC Load Power

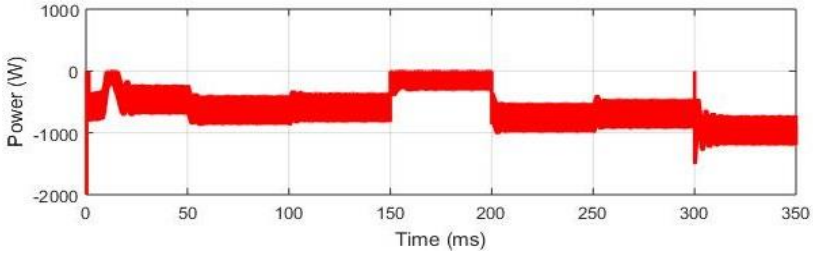

Fig. 16 ESU Power

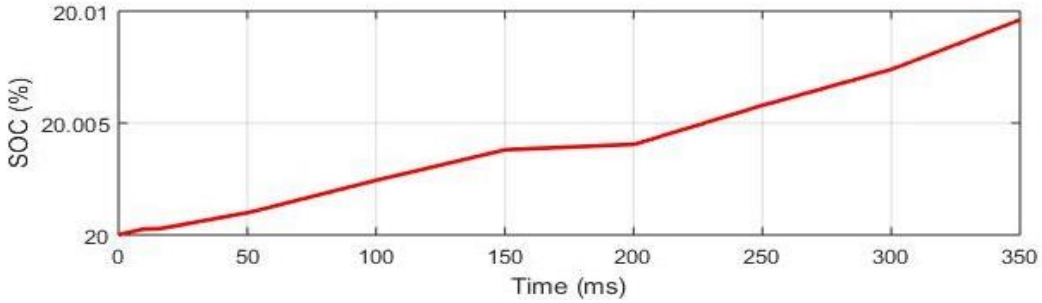

Fig. 17. ESU Battery SOC

The ESU power is represented by Fig. 16. The power is negative when charging and the battery power is positive during the discharge period. Since the SOC of ESU is less than the desired limit, the ESU battery is charging from 0 ms till 150 ms. The load power and PV generated power are same from 150 ms to 200 ms and hence, the ESU battery power is zero. Again, the ESU battery continue to charge from the PV generated power. The battery SOC of ESU is represented by Fig. 17.

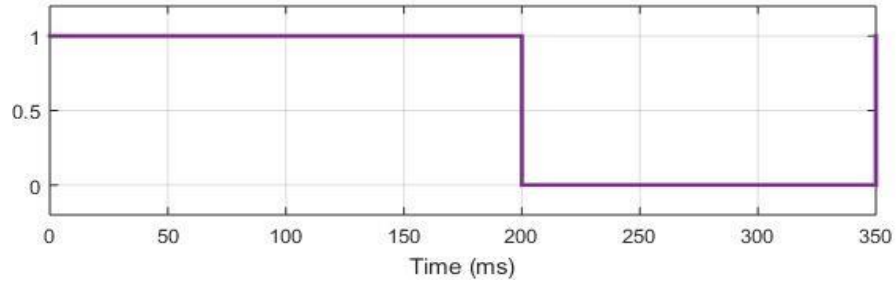

Fig. 18 Status of G2V Battery

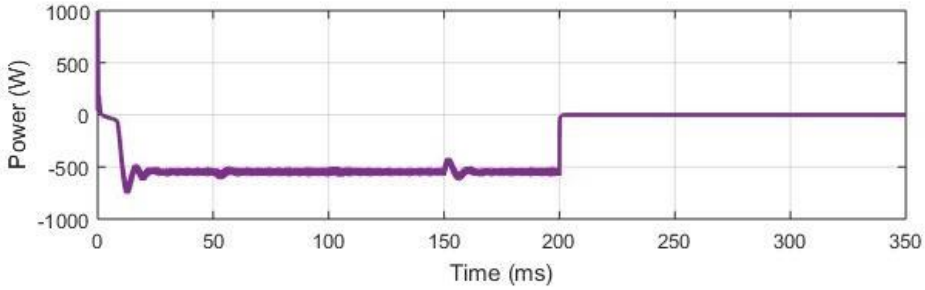

Fig. 19. G2V Battery Power

Fig. 16 shows the status of G2V battery. It can be seen from the figure that the G2V battery is connected to the grid for charging from 0 -200ms. The PV power is insufficient to meet the load power, ESU battery and G2V battery demand. Hence, the V2G battery is supplying energy to the grid in order to meet the requirement. Fig. 17 shows the G2V battery power. G2V battery is charging with a power of 500W between 0-200ms. The SOC of G2V battery and V2G battery are depicted in Fig. 20 and Fig. 21 respectively.

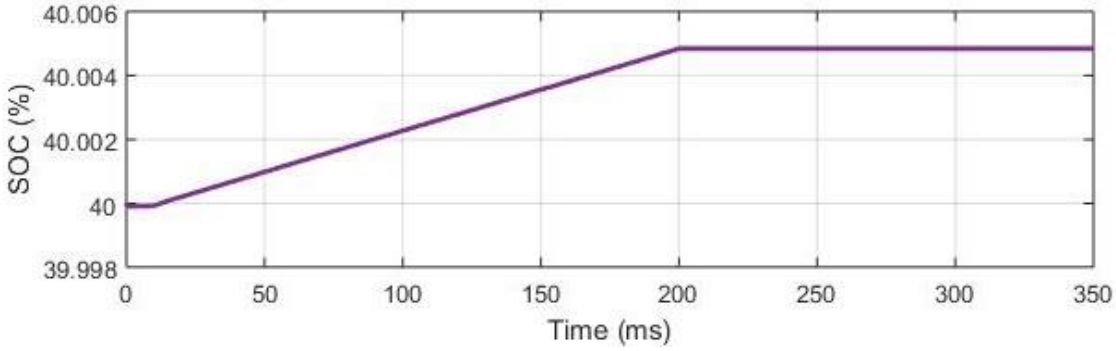

Fig. 20. G2V Battery SOC

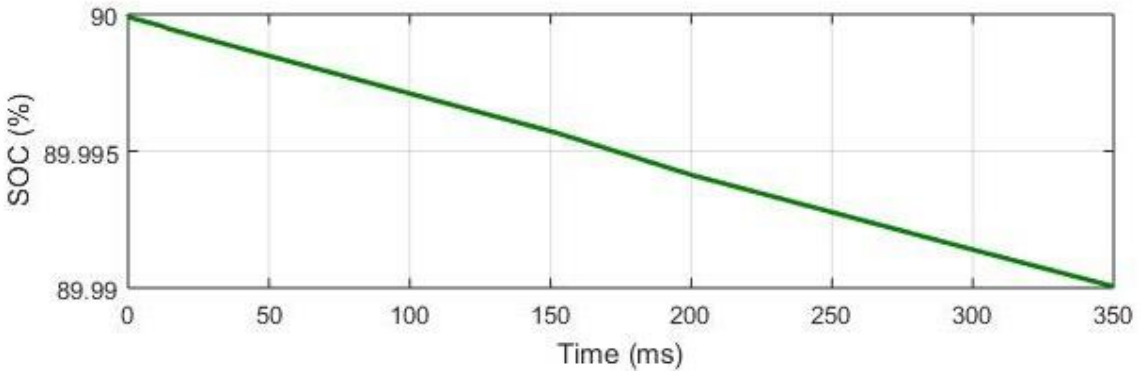

Fig. 21. V2G Battery SOC

It can be observed from fig. 21, V2G battery is discharging throughout the period to provide supplementary power along with the PV power to balance total power in the system. The EMS determines the charging and discharging of the ESU, G2V and V2G batteries, depending on the SOC and the power requirement of the system.

The variation of PV power, DC load, EV_g power, EV_v power and ESU power are tabulated in Table 7. It can be observed from this table that the total power in the grid is balanced by different sources according to the availability of source power and required power.

Table 7. Result Analysis

IRRADIATION (W/m^2)	**PV POWER (W)**	**DC LOAD (W)**	**EV_g POWER (W)**	**EV_v POWER (W)**	**ESU POWER (W)**
447	447	0	-500	601.3	-510.5
616	616	0	-500	602	-646.3
575	575	0	-500	600.4	-585.75
580	580	600	-500	757.4	-223.2
770	770	600	0	600.8	-745
705	705	600	0	608.2	-694.9
400	400	0	0	600.2	-990.2

Conclusion

A solar powered EV charging system with V2G and G2V configuration of EVs and back up battery ESU is discussed in this chapter. Design of various converters associated with the proposed system such as Interleaved Buck converter, Bi-directional Buck-Boost converter, Interleaved Boost converter are explained in detail. Ripple analysis of the conventional and

interleaved converter are carried out and the results are analyzed. The proposed system is built in MATLAB/Simulink and simulation is performed under different input and load conditions. The results obtained from the simulation studies for the selected input and load conditions confirm the effectiveness of EMS in maintaining the grid power by switching between different sources. The V2G, G2V operation is also realized.

Reference

[1] INTERNATIONAL ENERGY AGENCY, "Global EV Outlook 2021 - Accelerating ambitions despite the pandemic," *Glob. EV Outlook 2021*, p. 101, 2021, [Online].

[2] "Data & Statistics - INTERNATIONAL ENERGY AGENCY," 2021. https://www.iea.org/data-and-statistics.

[3] S. F. Tie and C. W. Tan, "A review of energy sources and energy management system in electric vehicles," *Renew. Sustain. Energy Rev.*, vol. 20, pp. 82–102, 2013, doi: 10.1016/j.rser.2012.11.077.

[4] T.-D. Nguyen, S. Li, W. Li, and C. C. Mi, "Feasibility study on bipolar pads for efficient wireless power chargers," in *2014 IEEE Applied Power Electronics Conference and Exposition - APEC 2014*, Mar. 2014, pp. 1676–1682, doi: 10.1109/APEC.2014.6803531.

[5] E. Akhavan-Rezai, M. F. Shaaban, E. F. El-Saadany, and A. Zidan, "Uncoordinated charging impacts of electric vehicles on electric distribution grids: Normal and fast charging comparison," in *2012 IEEE Power and Energy Society General Meeting*, Jul. 2012, pp. 1–7, doi: 10.1109/PESGM.2012.6345583.

[6] E. A. Nanaki, G. A. Xydis, and C. J. Koroneos, "Electric vehicle deployment in urban areas," *Indoor Built Environ.*, vol. 25, no. 7, pp. 1065–1074, Nov. 2016, doi: 10.1177/1420326X15623078.

[7] B. Battke, T. S. Schmidt, D. Grosspietsch, and V. H. Hoffmann, "A review and probabilistic model of lifecycle costs of stationary batteries in multiple applications," *Renew. Sustain. Energy Rev.*, vol. 25, pp. 240–250, Sep. 2013, doi: 10.1016/j.rser.2013.04.023.

[8] D. B. Richardson, "Electric vehicles and the electric grid: A review of modeling approaches, Impacts, and renewable energy integration," *Renew. Sustain. Energy Rev.*, vol. 19, pp. 247–254, Mar. 2013, doi: 10.1016/j.rser.2012.11.042.

[9] P. J. Tulpule, V. Marano, S. Yurkovich, and G. Rizzoni, "Economic and environmental impacts of a PV powered workplace parking garage charging station," *Appl. Energy*, vol. 108, pp. 323–332, Aug. 2013, doi: 10.1016/j.apenergy.2013.02.068.

[10] D. P. Birnie, "Solar-to-vehicle (S2V) systems for powering commuters of the future," *J. Power Sources*, vol. 186, no. 2, pp. 539–542, Jan. 2009, doi: 10.1016/j.jpowsour.2008.09.118.

[11] J. Traube, F. Lu, and D. Maksimovic, "Photovoltaic power system with integrated electric vehicle DC charger and enhanced grid support," in *2012 15th International Power Electronics and Motion Control Conference (EPE/PEMC)*, Sep. 2012, p. LS1d.5-1-LS1d.5-5, doi: 10.1109/EPEPEMC.2012.6397399.

[12] FK Tuffner MCW Kintner-Meyer FS Chassin K Gowri, "Utilizing Electric Vehicles to Assist Integration of Large Penetrations of Distributed Photovoltaic Generation," 2012.

[13] H.-M. Neumann, D. Schär, and F. Baumgartner, "The potential of photovoltaic carports to cover the energy demand of road passenger transport," *Prog. Photovoltaics Res. Appl.*, vol. 20, no. 6, pp. 639–649, Sep. 2012, doi: 10.1002/pip.1199.

[14] Hassan Fathabadi, *"Novel solar powered electric vehicle charging station with the capability of vehicle-to-grid",* Solar Energy, Vol. 142, pp. 136-143, 2017.

[15] Savio, D.A.; Juliet, V.A.; Chokkalingam, B.; Padmanaban, S.; Holm-Nielsen, J.B.; Blaabjerg, F., "*Photovoltaic Integrated Hybrid Microgrid Structured Electric Vehicle Charging Station and Its Energy Management Approach*", Energies, Vol. 12, pp. 168-196, 2019.

[16] Ashna Joseph, Jebin Francis, "*Design and Simulation of Two Phase Interleaved Buck Converter*", NCREEE, Vol. 4, 2015

[17] John, Riby& Mohammed S, Sheik & Zachariah, Richu, "*Variable step size Perturb and observe MPPT algorithm for standalone solar photovoltaic system*", IEEE International Conference on Intelligent Techniques in Control, Optimization and Signal Processing (INCOS), pp. 1-6, 2017.